agriculture

MDPI

Article

Effect of Cyclic Loading Treatment on the Compression Energy and Creep Properties of Machine-Harvested Seed Cotton

Ximei Wei [1,†], Meng Wang [1,2,†], Hongwen Zhang [1,2,*], Lei Wang [1,2], Xintian Du [1], Lixin Chen [1] and Shaohua Zhi [1]

[1] College of Mechanical Electrical Engineering, Shihezi University, Shihezi 832000, China; 20202009018@stu.shzu.edu.cn (X.W.); wangmeng@shzu.edu.cn (M.W.); wl_mac@shzu.edu.cn (L.W.); 20202109018@stu.shzu.edu.cn (X.D.); chenlixin@stu.shzu.edu.cn (L.C.); zsh@stu.shzu.edu.cn (S.Z.)
[2] Key Laboratory of Northwest Agricultural Equipment, Ministry of Agriculture and Rural Affairs, Shihezi 832000, China
* Correspondence: zhw_mac@shzu.edu.cn
† These authors contributed equally to this work.

Abstract: Machine-harvested seed cotton was taken as the research object to further clarify its creep performance, minimize its power consumption during the loading process, and obtain a better loading method. The uniaxial compression creep test was carried out using the Instron universal material test bench to apply cyclic loading treatment. The test factors included cyclic loading times, cyclic stress peak, and cyclic loading frequency. The energy consumption curve of the machine-harvested seed cotton during cyclic loading was obtained through OriginPro 2019b software, and its energy change law was analyzed. Creep strain was divided into two parts, namely, initial creep strain and creep strain increment, to elucidate the creep mechanism. The Burgers model was chosen to describe the creep strain increment. Results show that machine-harvested seed cotton exhibits energy consumption hysteresis during cyclic loading. The compression energy rapidly decreases with increasing cyclic loading times and then stabilizes. Meanwhile, the compression energy increases with increasing cyclic stress peak and cyclic loading frequency. The creep strain mechanism is also the same, which first rapidly increases and then levels off. Cyclic loading times, cyclic stress peak, and cyclic loading frequency have different effects on creep strain increment, instantaneous elastic modulus, hysteresis elastic modulus, viscosity coefficient, delay time, and relative deformation index. Finally, disregarding power consumption and interaction, extending the cyclic loading time, and increasing the cyclic stress peak while simultaneously minimizing the cyclic loading frequency can reduce the relative deformation index in the creeping stage. Accordingly, the deformation retention ability in the creep is improved, but the compression energy in the cyclic loading increases. The results can provide theoretical and data support for studying the theoretical basis of the rheological properties of machine-harvested seed cotton, the design of seed cotton baling devices, and the study of bale (mold) forming quality.

Keywords: cyclic loading; machine-harvested seed cotton; compression energy; creep property; relative deformation index

Citation: Wei, X.; Wang, M.; Zhang, H.; Wang, L.; Du, X.; Chen, L.; Zhi, S. Effect of Cyclic Loading Treatment on the Compression Energy and Creep Properties of Machine-Harvested Seed Cotton. *Agriculture* **2024**, *14*, 239. https://doi.org/10.3390/agriculture14020239

Received: 2 January 2024
Revised: 25 January 2024
Accepted: 26 January 2024
Published: 31 January 2024

1. Introduction

Cotton is an essential strategic reserve material in China and one of the major cash crops in Xinjiang [1]. Xinjiang has consistently maintained its leading position in China for 28 consecutive years in terms of cotton production and planting area [2]. Moreover, the adoption of machine harvesting for cotton in Xinjiang is a significant trend. Round mold baling cotton pickers have emerged as the predominant trend in the technological development of cotton pickers due to their advantages, such as high compression density, low operating cost, and high transportation and storage efficiency [3]. Although compression plays a vital role in the cotton picker baling process, field trials have revealed issues with machine-harvested seed cotton. These problems include bale cracking, loose bales,

and nonformation after baling. Researchers have shown that fiber materials exhibit viscoelastic behavior during deformation [4]. Seed cotton is an agricultural fiber material [5] that exhibits viscoelastic behaviors, including stress relaxation, creep, and springback, during the postprocessing steps, such as compression molding and baling. These behaviors contribute to size and shape changes in the bales relative to their initial baling, resulting in poor dimensional stability and even potential damage to the bale. Hence, the rheological characteristics of stress relaxation, creep, and springback in seed cotton play a crucial role in optimization relevant to baling equipment parameters, power consumption, and bale dimensional stability [6]. Meanwhile, modern computing tools are known for their speed, efficiency, and cost-effectiveness. When these modern computational tools are applied to seed cotton, a notable challenge arises due to the relatively limited availability of data on the rheological properties of the material. Accordingly, the rheological properties of seed cotton must be explored. Kong et al. [6,7] studied the compression and stress relaxation characteristics of seed cotton and obtained the influence of moisture content and feeding quality on the compression and stress relaxation model, which can provide a theoretical reference for the compression process of seed cotton and the optimal design of the baling mechanism.

Scholars have conducted less research on the creep characteristics of machine-harvested seed cotton. Hardin used the Burgers model to study the compression and creep characteristics of scattered low-density (64–128 kg/m^3) cotton. The results showed that the number of compression (15 times) had an effect on the compression density [8]. However, the density of the existing harvesting and packaging machine could reach 199–240 kg/m^3 [9]. Research results on other agricultural materials are more abundant, and the theory is more well established [10–12]. Xiao et al. [13] outlined the creep properties of rice seedlings by using the Burgers model and showed that different load levels have an influence on creep parameters. The creep strain rate under constant and cyclic humidity conditions was linearly related to the applied load level [11]. Graham et al. [14] used a nonlinear viscoelastic model to simulate the creep process of grass materials and noted that the parameters in the model were related to the stress, material type, and moisture content. Nielsen et al. [15] proposed a nonlinear Maxwell model to simulate the compression and stress relaxation behavior of agricultural materials during compression and found that the compression speed was related to the model parameters. Du et al. [16] established a five-element Maxwell mathematical model. The parameter optimization tests indicated that the specific energy consumption was minimal at a moisture content of 57%, providing a theoretical foundation for the optimal design of low-density straw block compression equipment and the required energy consumption.

The superimposed vibration on the biomass compression process could increase the stress relaxation rate and minimize the stress relaxation time and residual stress inside the forming block, which could minimize the compression resistance and energy consumption of recompression and improve the product quality and productivity [17]. Moreover, continuous compression can remove air between fibers and promote fiber densification, and the energy consumption of each layer exponentially increases with the compression volume [18]. The relaxation ratio of maize straw compression molding was 1.2–1.5 at a compression force of 6.22 MPa, a compression time of 2–6 times, and a compression speed of 128–337 mm·min^{-1} [19].

In summary, the loading method of agricultural materials affects not only their power consumption during compression but also their subsequent rheological properties, such as stress relaxation, creep, and springback. A single-factor experiment was conducted to investigate the influence of the cyclic loading method on the energy consumption and creep performance of machine-harvested seed cotton, minimize the power consumption during the loading process of seed cotton, and obtain a better loading method of seed cotton. The effects of cyclic loading times, cyclic stress peak, and cyclic loading frequency on the energy consumption of the cyclic loading stage and the creep performance of the creeping stage of machine-harvested seed cotton were investigated through a combination of experimental

and theoretical methods. The experimental results can provide academic and data support for studying the rheological characteristics of seed cotton, designing the seed cotton baling device, and clarifying the seed cotton forming mechanism and the molding quality of the molding bale (mold).

2. Materials and Methods

2.1. Experimental Materials

The samples were taken from the experimental field of Shihezi University and sown on 12 May 2022. A total of 1000 cotton plants with remarkable growth and no disease or insect damage were selected. Thereafter, samples were cut from the roots of the cotton plants with fruiting shears, sampled and wrapped in black plastic bags for single plant sealing, and transported back to the laboratory on 8 October 2022. Finally, the samples were harvested through the self-built cotton-picking performance test bench (Shihezi University, Shihezi, China) and stored in a black sealed bag. The schematic diagram of the seed cotton-picking process is shown in Figure 1.

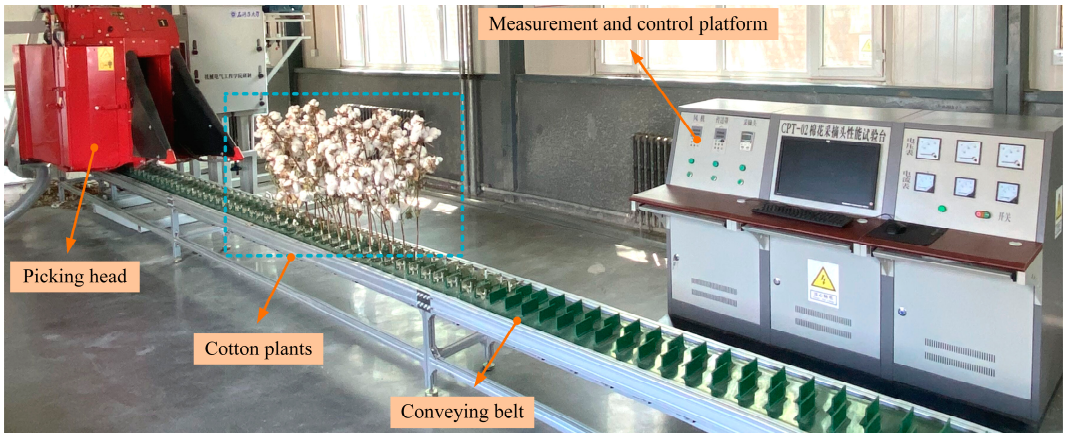

Figure 1. Schematic of the seed cotton picking process.

2.2. Test Apparatus and Equipment

An Instron E1000 universal material testing machine (maximum static load of 700 N; maximum stroke of 60 mm; Instron Worldwide Headquarters 825 University Ave, Norwood, MA, USA), a Shengbo SB 5002–R precision electronic balance (range: 0–500 g; accuracy: 0.01 g; Shengbo Electronics Co., Ltd., Foshan, China), an MA45 moisture meter (range: 0–45 g; accuracy: 1 mg; readability: 0.01%; Beijing United Keli Technology Co., Ltd., Beijing, China), a DHG–9070A drying oven (Shanghai Yiheng Technology Ltd., Shanghai, China), a pressure head, a homemade base plate, a homemade compression chamber, and a sealing bag were used in the experiment.

This experiment used machine-harvested seed cotton as the research object by using a homemade compression chamber and plate mounted on the Instron E1000 Universal Material Testing Machine. The universal material testing machine provided compression power, and the test was completed with the compression head on the Instron E1000 Universal Material Testing Machine. The diameter of the circular indenter was 50 mm, and the corresponding compression chamber was 52 mm in diameter and 4 mm in thickness. The material used was a seamless stainless-steel pipe to ensure the stability of the piston's forward direction. Given that the maximum compression stroke of the Instron E1000 Universal Material Testing Machine was 60 mm, the depth of the chamber was 60 mm, which could fit well with the chamber. The wall inside the chamber was polished to minimize the influence of the frictional resistance of the wall during compression. The bottom of the compression chamber was in the form of a removable plate, which was connected to the box through a groove to ensure that the material could be easily unloaded

after compression. The compression process of each component connection, installation mode, and working state is shown in Figure 2.

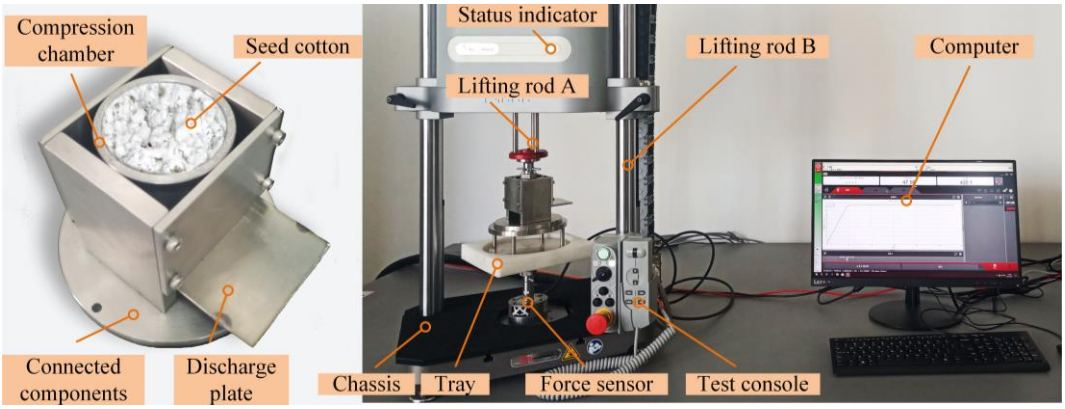

Figure 2. Diagram of the compression process of the machine-harvested cotton.

2.3. Experimental Factors

The stress and stress change law in the compression molding process of agricultural materials are influenced by various factors, such as moisture content, trash content, compression time, cross-sectional shape, initial density, and load [20,21]. The baling process of the machine-harvested seed cotton could be regarded as a series of multiple successive compressions. In consideration of the pre-experimental findings and a review of existing literature, the cyclic loading times were chosen to be 5, 10, 15, 20, and 25 times for a total of five levels [8,18,22]. The pre-experiments showed that the machine-harvested seed cotton was compressed to 300 kg m^{-3} when the cotton seeds were broken, and the corresponding pressure at this time was 0.34 MPa [23]. The existing baling machines in the market had a baling density range of approximately 180–220 kg m^{-3}, and the corresponding pressure at this time was 0.09 MPa. Accordingly, the selected load intervals were 180, 210, 240, 270, and 300 N for a total of five levels, corresponding to peak stress levels of 0.085, 0.099, 0.113, 0.127, and 0.141 MPa, respectively. Given that the bale diameter range was 0.5–2.4 m in the seed cotton baling process, the baling line speed of the seed cotton baling belt was 1.3 m s^{-1}, and the compression frequency was selected to be 0.2, 0.4, 0.6, 0.8, and 1.0 Hz for a total of five levels. Therefore, this study chose three influencing factors, namely, cyclic loading time, cyclic stress peak, and cyclic loading frequency, to conduct a single-factor experimental study on the compression creep characteristics of the machine-harvested seed cotton to investigate the cyclic loading energy consumption and compression creep law of the machine-harvested seed cotton during the test.

2.4. Experimental Process

The circular indenter and the compression test bench were installed on the Instron E1000 universal material testing machine. After the operation was stabilized, the same quality of the machine-harvested seed cotton was randomly and uniformly fed. After lifting the pressure head to the calibration position before the test, the creep test parameters were set according to the above-mentioned test level. The force control method was adopted for the test. The indenter was compressed downward at the loading speed of v = 10 N·s^{-1}. When the cyclic stress peak rose to σ, the system was unloaded, and the indenter was lifted up, constituting one cycle. The set N cycles took t_1 to complete. Thereafter, the system was loaded at v = 10 N·s^{-1}. When cyclic stress peak rose to σ, the creep was maintained until the time was t*. The full process curve of the specimen test is shown in Figure 3.

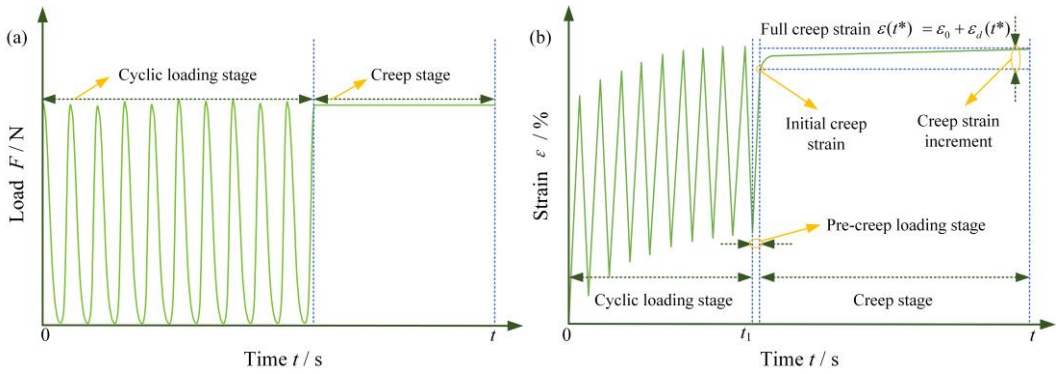

Figure 3. Schematic of the whole process curve: (**a**) load and (**b**) strain changing with time.

3. Results and Discussion

Each group of tests was repeated five times, and the data obtained were divided into two parts, namely, cyclic loading and creep phases, to analyze and characterize the energy changes during cyclic loading, the creep characteristics, and the ability of the machine-harvested seed cotton to maintain the initial creep strain during creep.

3.1. Cyclic Loading Phase

Given that the fiber density of the machine–harvested seed cotton in the 1st cycle was not uniform, more air was observed, and the curve unevenly changed during the compression process; the data are shown from the second cycle [24]. Figure 4a shows that in the force–displacement curve of the whole cyclic loading process, machine-harvested seed cotton exhibits hysteresis characteristics under the action of cyclic loading, which is consistent with the results after cyclic loading of rice grains [25]. The area enclosed by each hysteresis loop gradually decreases with the increase in the cyclic loading times, and the curves overlap after the fifth cycle. Therefore, the test treated each of the five cyclic loading curves as a group and analyzed the repetition period and characteristic parameters of each group of cyclic loading curves.

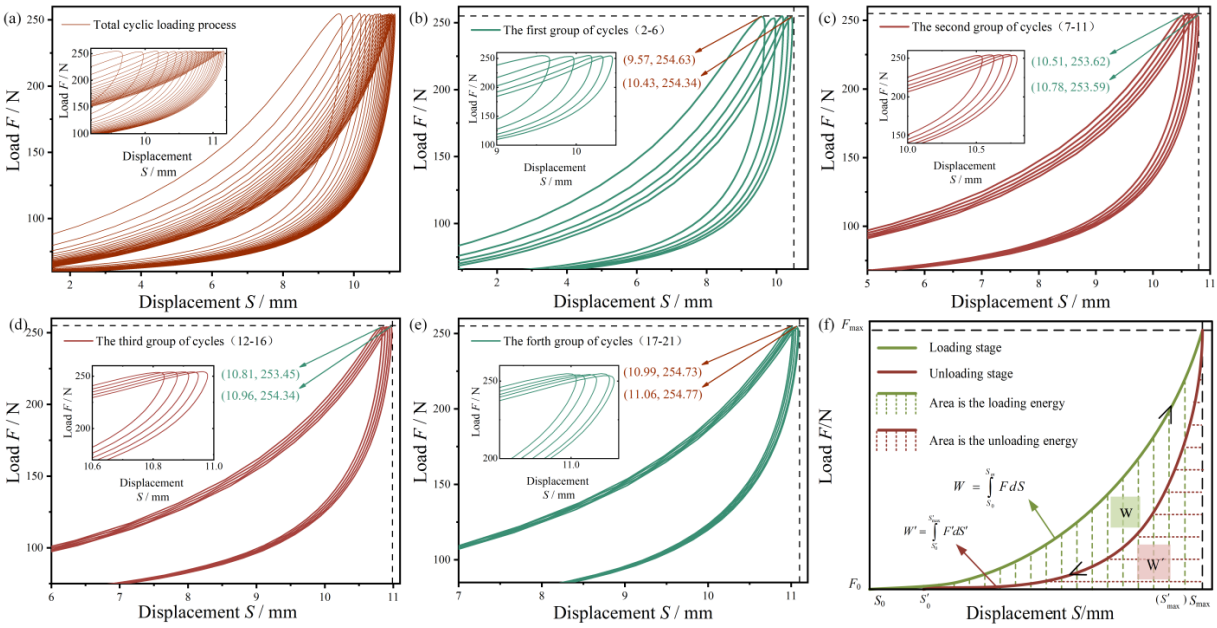

Figure 4. Load-displacement diagram of the whole cyclic loading process (**a**), the first group of cycles (**b**), the second group of cycles (**c**), the third group of cycles (**d**), and the fourth group of cycles (**e**); and schematic of the energy absorbed by the seed cotton (**f**) in the cyclic loading stage.

The first four groups of cyclic loading curves reveal that the hysteresis curves of the machine-harvested seed cotton are consistent with the different cyclic loading times (Figure 4b–e). The hysteresis curves of the machine-harvested seed cotton significantly deviate with increased cyclic loading times. The first group of curves (Figure 4b, i.e., 2nd–6th cyclic loading curves) remarkably deviate, with a displacement difference of 0.88 mm. The second and third groups of curves (Figure 4c,d, i.e., the 7th–11th and 12th–16th cyclic loading curves, respectively) remarkably deviate, with displacement differences of 0.27 and 0.15 mm, respectively. The deviation of the fourth group of curves (Figure 4e, i.e., 17th–21st cyclic loading curves) is the smallest, and the hysteresis curves almost overlap, with an intragroup displacement difference of 0.07 mm, which is due to the plastic deformation and accumulation of the machine-harvested seed cotton during the cyclic loading process.

The area enclosed by each hysteresis loop represents the energy the machine-harvested seed cotton absorbed in one loading-and-unloading cycle. In summary, increasing the cycle loading time results in a reduction in the area enclosed by the hysteresis loop, which rapidly decreases, then slowly decreases, and finally remains in a relatively stable state. Specifically, the less energy absorbed, and the more energy lost in the cyclic loading process of the machine-harvested seed cotton, the smaller the displacement difference within the group in the subsequent cycle process. Accordingly, the first two groups of cycles (i.e., 2–11 cycles of the loading process) were selected for the energy change in the cyclic loading process of the machine-harvested seed cotton for further analysis. Meanwhile, the energy absorbed by the machine-harvested seed cotton during the loading phase (later expressed as compression energy) was analyzed for one machine-harvested seed cotton cyclic loading cycle as follows (Figure 4f):

$$W = \int_{S_0}^{S_{\max}} F dS \tag{1}$$

where W is the energy absorbed by one cycle of seed cotton loading (compression energy), S_0 is the moment of the beginning of loading (end of unloading) in one cycle, $S_{\max}$ is the time of the end of loading (beginning of unloading) in one cycle, and F is the loading phase load.

The energy absorbed by machine-harvested seed cotton during the unloading phase is:

$$W' = \int_{S'_0}^{S'_{\max}} F' dS' \tag{2}$$

where W' is the energy absorbed by the unloading of seed cotton in one cycle, S'_0 is the moment of the end of unloading in one cycle, $S'_{\max}$ is the time of the beginning of unloading in one cycle, and F' is the load of the unloading phase.

3.1.1. Effect of Cycle Loading Number on the Compression Energy of Machine-Harvested Seed Cotton

The trend of the compression energy of the machine-harvested seed cotton with the cyclic loading time is shown in Figure 5. Figure 5a,b depict that the trend of the compression energy of the machine-harvested seed cotton under different cyclic loading times can be divided into three stages. The compression energy rapidly decreases in the first stage, slowly decreases in the second stage, and stabilizes in the third stage. Under the same cyclic stress peak and cyclic loading frequency conditions, the change law of the machine-harvested seed cotton compression energy can be expressed as an exponential function ($R^2 \geq 0.91$) with increasing cyclic loading times. This result reveals that the compression energy of the machine-harvested seed cotton under different cyclic loading times first rapidly decreases and then stabilizes because the seed cotton in the first stage is loose and has sufficient air. The friction inside the seed cotton and between the seed cotton and

the chamber is small and compressible. The air is gradually discharged as the pressure head descends, and the force and displacement are increased, thus requiring considerable compression energy. In the second stage, more plastic deformation is gradually produced with increased cyclic loading times. The seed cotton density increases, the internal voids decrease, and the friction inside the seed cotton and between the seed cotton and the chamber increases. Accordingly, a small displacement requires a large force, resulting in a small compression energy at this stage. In the third stage, more plastic deformation is produced, the seed cotton reaches a higher density, its internal fibers are bonded to each other, the internal clearances are extremely small, the compressibility is poor, and the material is a solid material. Accordingly, the pressure can instantly increase during the compression process, and a minimal displacement requires a large force, resulting in a smaller compression energy. The overall trend of energy in the unloading phase is the same as that in the loading phase (Figure 5c). Thus, only the loading phase is subsequently analyzed.

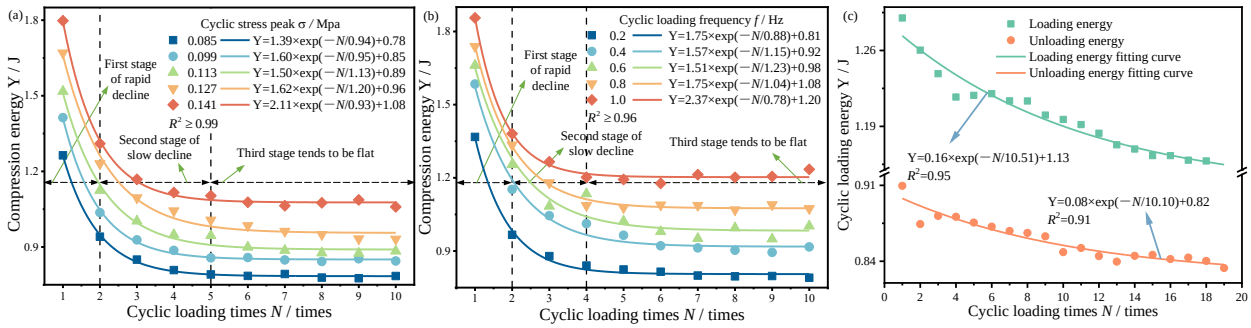

Figure 5. Variation in compression energy with cyclic loading times under different cyclic stress peaks (**a**) and cyclic loading frequencies (**b**); comparison curves of compression energy and unloading energy corresponding to different cyclic loading times (**c**).

3.1.2. Effect of Cyclic Stress Peak on the Energy Consumption of Machine-Harvested Seed Cotton

Figure 6 shows the required compression energy in the cyclic loading process of the machine-harvested seed cotton for the different cyclic stress peaks. The needed compression energy of the machine-harvested seed cotton increases with the increase in the cyclic stress peak. This relationship is due to the exponential growth of the seed cotton compression force and compression density in the single seed cotton compression process under the same loading frequency and cyclic loading times [23].

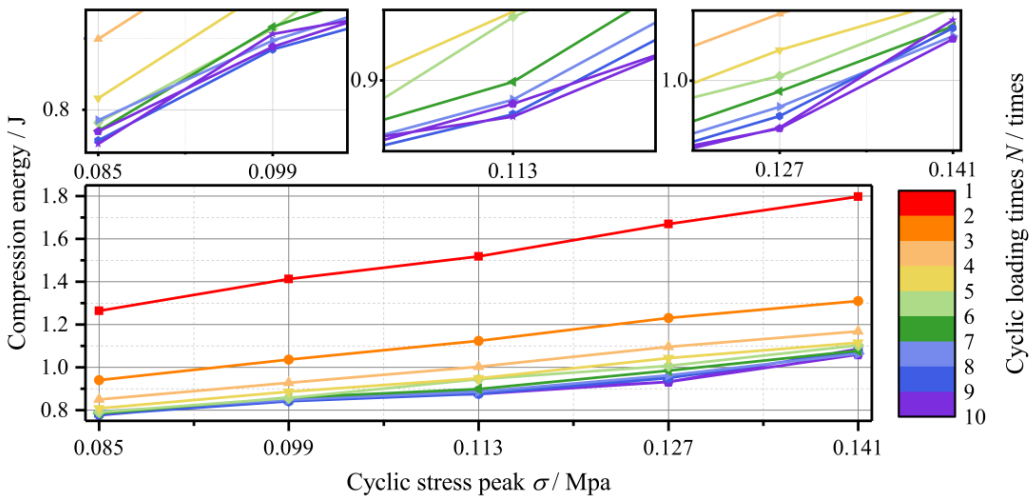

Figure 6. Change trend of compression energy with cyclic stress peak.

Increasing the cyclic stress peak results in the formation of more fiber bonds within the machine-harvested seed cotton. This scenario results in greater plastic deformation and higher seed cotton density. Moreover, the air between the cotton fibers decreases, the seed cotton inside is tighter, and the friction forces inside the seed cotton and between it and the chamber increase, making the seed cotton less likely to be compressed. The final part of the survey revealed an increase in the required compression energy during the machine-harvested seed cotton compression process. Similar observations were made by Du et al. [26], who showed that the higher the compression force needed for the forming process, the greater the energy consumed.

3.1.3. Effect of Cyclic Loading Frequency on the Energy Consumption of Machine-Harvested Seed Cotton

Figure 7 shows the trend of the required compression energy for the machine-harvested seed cotton under different cyclic loading frequencies. When the cyclic loading times and stress peaks are the same, the required compression energy of the machine-harvested seed cotton increases with the increase in the cyclic loading frequency. This relationship occurs because the higher the cyclic loading frequency is, the faster the compression speed, and the better the air resistance will be. When the time to unload and return after each compression of the machine-harvested seed cotton is short, the internal bonding of the fibers cannot be popped open to be compressed again, resulting in a closer bond. This bond results in more significant deformation, increasing the seed cotton density. Moreover, the internal friction of the seed cotton and the friction between the seed cotton and the chamber increase, indicating that the required compression energy of the machine-harvested seed cotton in the process increases.

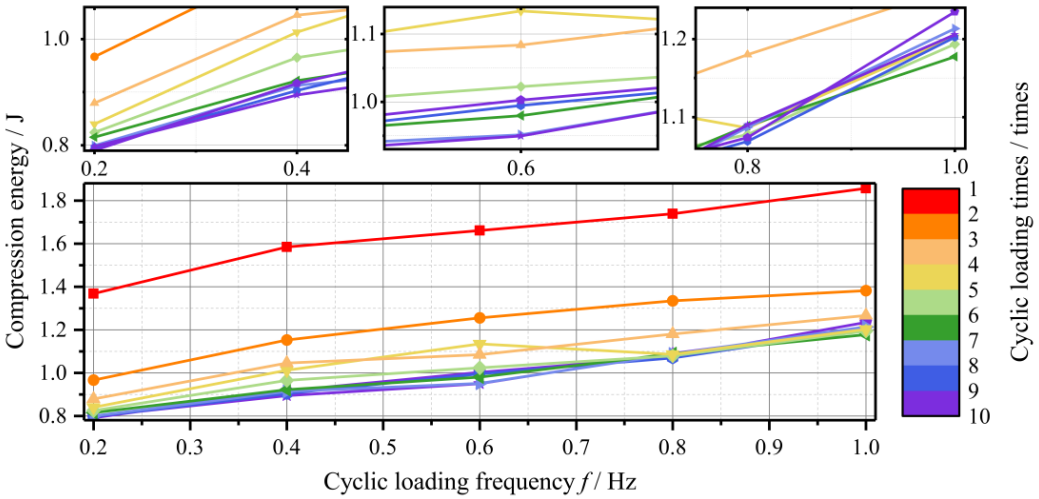

Figure 7. Change trend of the compression energy with cyclic loading frequency.

3.2. Creep Stage

The full creep strain $\varepsilon(t^*)$ of the machine-harvested seed cotton was divided into two parts for further analysis of the effect of the cyclic loading method on the creep performance of the machine-harvested seed cotton: initial creep strain ε_0 and creep strain increment $\varepsilon_d(t^*)$:

$$\varepsilon(t*) = \varepsilon_0 + \varepsilon_d(t*), \tag{3}$$

where ε_0 is the initial creep strain, which is only related to the loading history before creep at the same stress level and not related to the creep time; and $\varepsilon_d(t^*)$ is the creep strain increment, which indicates the increase in deformation with the creep time during creep and is related to the creep time.

The creep strain increment is particularly important for the creep characteristics of the machine-harvested seed cotton. Agricultural materials are typically described by a

four-element Burgers model [27]. The model consists of a spring (E_1) in series with a damper (η_1) and a spring (E_2) and a damper (η_2) in parallel. Therefore, the four-element Burgers model was used in this study to characterize further the seed cotton creep strain increment law to elucidate the effect of test factors on the viscoelastic mechanical index of the strain increment in the creep phase of the machine-harvested seed cotton, which is expressed as follows:

$$\varepsilon = \frac{\sigma}{E_1} + \frac{\sigma}{E_2}\left(1 - e^{-t/\tau_r}\right) + \frac{\sigma}{\eta_1}t, \quad (4)$$

where σ is stress, MPa; ε is strain; t is creep time, s; E_1 is instantaneous elasticity modulus, MPa; η_1 is viscosity coefficient, MPa·s; E_2 is the hysteresis modulus of elasticity, MPa; and τ_r is delay time, s.

The relative deformation index β was introduced to characterize the ability of the machine-harvested seed cotton to maintain the initial deformation during creep, and its mathematical expression is as follows:

$$\beta = \frac{\varepsilon(t^*) - \varepsilon_0}{\varepsilon_0} \times 100\% = \frac{\varepsilon_d(t^*)}{\varepsilon_0} \times 100\%. \quad (5)$$

The smaller the relative deformation index β is, the better the ability of the machine-harvested seed cotton to maintain the initial deformation during creep, and the better the dimensional stability will be. β = 0 when the creep time t^* = 0, indicating that no deformation is generated relative to the initial creep strain.

OriginPro 2019b software was used to fit the creep strain increments at different machine-harvested seed cotton factor levels in accordance with Equation (4). The fitting results are shown in Table 1, which is at the end of the paper. The data are expressed as the mean ± standard deviation. The correlation coefficient $R^2 \geq 0.97$ indicates that the model fits well, and the Burgers model is suitable for describing the creep strain increments of the machine-harvested seed cotton. The correlations of the creep strain increments corresponding to each factor are shown in Table 2. Meanwhile, 0.05 was selected for the significance test to investigate the influence of each factor on the law and characteristics of the creep strain increment [28]. The fitted parameters were analyzed by ANOVA with IBM SPSS Statistics 26 software.

Table 1. Fitting parameters of the creep strain increment model.

Experimental Factor	Level of Factor	Instantaneous Elasticity Modulus E_0/MPa	Hysteretic Elasticity Modulus E_r/MPa	Coefficient of Viscosity η/(MPa·s)	Relaxation Time τ_r/s	R^2
Cyclic loading times/times	5	0.27 ± 0.00	0.17 ± 0.00	238.10 ± 1.63	21.28 ± 0.08	0.98
		0.28 ± 0.00	0.16 ± 0.00	370.44 ± 4.26	21.94 ± 0.08	0.98
		0.33 ± 0.00	0.16 ± 0.00	423.84 ± 4.68	19.62 ± 0.07	0.98
		0.36 ± 0.00	0.19 ± 0.00	466.79 ± 5.51	20.53 ± 0.08	0.97
		0.38 ± 0.00	0.18 ± 0.00	220.53 ± 1.26	21.53 ± 0.08	0.98
	10	0.9 ± 0.00	0.24 ± 0.00	119.64 ± 0.28	27.30 ± 0.09	0.99
		0.41 ± 0.00	0.22 ± 0.00	196.01 ± 0.82	21.83 ± 0.08	0.99
		0.46 ± 0.00	0.21 ± 0.00	233.52 ± 1.30	23.53 ± 0.09	0.98
		0.50 ± 0.00	0.23 ± 0.00	246.96 ± 1.27	22.60 ± 0.08	0.98
		0.48 ± 0.00	0.22 ± 0.00	322.11 ± 2.30	21.51 ± 0.08	0.98
	15	1.17 ± 0.01	0.3 ± 0.00	135.23 ± 0.35	31.59 ± 0.11	0.99
		0.67 ± 0.00	0.29 ± 0.00	317.02 ± 2.20	29.06 ± 0.12	0.98
		0.58 ± 0.00	0.27 ± 0.00	257.50 ± 1.43	27.39 ± 0.11	0.99
		0.70 ± 0.00	0.29 ± 0.00	425.20 ± 3.29	26.84 ± 0.10	0.98
		0.56 ± 0.00	0.26 ± 0.00	252.83 ± 1.30	25.55 ± 0.10	0.99

Table 1. *Cont.*

Experimental Factor	Level of Factor	Instantaneous Elasticity Modulus E_0/MPa	Hysteretic Elasticity Modulus E_r/MPa	Coefficient of Viscosity η/(MPa·s)	Relaxation Time τ_r/s	R^2
	20	0.64 ± 0.00	0.27 ± 0.00	288.92 ± 1.52	25.54 ± 0.09	0.99
		0.64 ± 0.00	0.29 ± 0.00	314.85 ± 2.18	30.02 ± 0.12	0.98
		0.70 ± 0.00	0.28 ± 0.00	255.14 ± 1.17	25.51 ± 0.09	0.99
		0.85 ± 0.00	0.33 ± 0.00	422.66 ± 3.19	30.72 ± 0.11	0.99
		0.63 ± 0.00	0.29 ± 0.00	241.41 ± 1.13	23.44 ± 0.10	0.98
	25	0.63 ± 0.00	0.27 ± 0.00	309.07 ± 1.90	26.57 ± 0.10	0.99
		0.97 ± 0.00	0.31 ± 0.00	929.47 ± 9.05	22.07 ± 0.06	0.99
		0.64 ± 0.00	0.29 ± 0.00	381.27 ± 2.54	25.40 ± 0.09	0.98
		0.90 ± 0.00	0.35 ± 0.00	281.64 ± 0.93	20.20 ± 0.07	0.99
		0.64 ± 0.00	0.30 ± 0.00	566.91 ± 5.55	25.64 ± 0.10	0.98
Cyclic stress peak σ/MPa	0.085	0.74 ± 0.00	0.18 ± 0.00	61.87 ± 0.11	29.74 ± 0.09	1.00
		0.33 ± 0.00	0.16 ± 0.00	68.99 ± 0.15	24.66 ± 0.09	0.99
		0.44 ± 0.00	0.17 ± 0.00	105.23 ± 0.30	25.23 ± 0.08	0.99
		0.41 ± 0.00	0.14 ± 0.00	185.29 ± 0.83	22.65 ± 0.06	0.99
		0.32 ± 0.00	0.14 ± 0.00	59.89 ± 0.12	23.46 ± 0.08	0.99
	0.099	0.44 ± 0.00	0.18 ± 0.00	83.08 ± 0.18	27.29 ± 0.09	0.99
		0.54 ± 0.00	0.22 ± 0.00	89.87 ± 0.21	31.28 ± 0.11	0.99
		0.44 ± 0.00	0.19 ± 0.00	80.12 ± 0.16	28.64 ± 0.09	1.00
		0.52 ± 0.00	0.21 ± 0.00	95.32 ± 0.26	33.96 ± 0.12	0.99
		0.53 ± 0.00	0.21 ± 0.00	70.69 ± 0.12	31.08 ± 0.10	1.00
	0.113	0.53 ± 0.00	0.22 ± 0.00	101.33 ± 0.27	33.11 ± 0.12	0.99
		0.70 ± 0.00	0.25 ± 0.00	81.14 ± 0.14	34.00 ± 0.10	1.00
		0.68 ± 0.00	0.26 ± 0.00	75.25 ± 0.12	34.59 ± 0.11	1.00
		0.63 ± 0.00	0.22 ± 0.00	73.12 ± 0.14	35.84 ± 0.12	1.00
		0.78 ± 0.00	0.25 ± 0.00	89.50 ± 0.16	34.49 ± 0.11	1.00
	0.127	1.01 ± 0.00	0.3 ± 0.00	79.45 ± 0.10	35.78 ± 0.1	1.00
		1.09 ± 0.00	0.29 ± 0.00	112.62 ± 0.21	36.16 ± 0.1	1.00
		0.80 ± 0.00	0.28 ± 0.00	112.27 ± 0.24	34.05 ± 0.11	1.00
		0.81 ± 0.00	0.24 ± 0.00	92.04 ± 0.19	40.14 ± 0.11	1.00
		1.04 ± 0.01	0.29 ± 0.00	74.72 ± 0.10	32.75 ± 0.11	1.00
	0.141	0.90 ± 0.00	0.28 ± 0.00	155.34 ± 0.50	40.01 ± 0.12	1.00
		1.16 ± 0.00	0.31 ± 0.00	87.46 ± 0.12	35.45 ± 0.10	1.00
		1.27 ± 0.01	0.32 ± 0.00	106.35 ± 0.17	36.54 ± 0.10	1.00
		1.34 ± 0.01	0.33 ± 0.00	107.22 ± 0.15	34.12 ± 0.09	1.00
		1.08 ± 0.00	0.33 ± 0.00	116.36 ± 0.33	46.04 ± 0.18	1.00
Cyclic loading frequency f/Hz	0.2	1.44 ± 0.01	0.39 ± 0.00	101.41 ± 0.14	38.52 ± 0.11	1.00
		1.33 ± 0.01	0.36 ± 0.00	98.27 ± 0.16	40.57 ± 0.13	1.00
		1.26 ± 0.01	0.36 ± 0.00	101.66 ± 0.22	40.93 ± 0.17	1.00
		1.42 ± 0.01	0.36 ± 0.00	104.31 ± 0.21	43.09 ± 0.15	1.00
		1.34 ± 0.01	0.35 ± 0.00	106.52 ± 0.24	42.09 ± 0.16	1.00
	0.4	0.83 ± 0.00	0.26 ± 0.00	79.58 ± 0.15	38.15 ± 0.13	1.00
		0.88 ± 0.00	0.28 ± 0.00	106.22 ± 0.19	34.79 ± 0.10	1.00
		0.79 ± 0.00	0.25 ± 0.00	95.88 ± 0.21	37.19 ± 0.12	1.00
		0.81 ± 0.00	0.25 ± 0.00	82.31 ± 0.15	36.94 ± 0.11	1.00
		0.85 ± 0.00	0.26 ± 0.00	88.84 ± 0.17	37.44 ± 0.11	1.00
	0.6	0.62 ± 0.00	0.21 ± 0.00	69.43 ± 0.12	33.49 ± 0.10	1.00
		0.65 ± 0.00	0.22 ± 0.00	61.24 ± 0.08	30.00 ± 0.09	1.00
		0.63 ± 0.00	0.21 ± 0.00	71.38 ± 0.12	33.80 ± 0.10	1.00
		0.62 ± 0.00	0.22 ± 0.00	74.31 ± 0.13	33.86 ± 0.10	1.00
		0.63 ± 0.00	0.23 ± 0.00	81.05 ± 0.15	33.08 ± 0.10	1.00

Table 1. *Cont.*

Experimental Factor	Level of Factor	Instantaneous Elasticity Modulus E_0/MPa	Hysteretic Elasticity Modulus E_r/MPa	Coefficient of Viscosity η/(MPa·s)	Relaxation Time τ_r/s	R^2
	0.8	0.53 ± 0.00	0.20 ± 0.00	61.68 ± 0.10	30.75 ± 0.10	1.00
		0.53 ± 0.00	0.20 ± 0.00	66.40 ± 0.11	31.53 ± 0.10	1.00
		0.55 ± 0.00	0.22 ± 0.00	67.27 ± 0.11	32.46 ± 0.10	1.00
		0.50 ± 0.00	0.20 ± 0.00	64.40 ± 0.10	31.21 ± 0.10	1.00
		0.49 ± 0.00	0.19 ± 0.00	67.48 ± 0.12	31.49 ± 0.10	1.00
	1.0	0.46 ± 0.00	0.19 ± 0.00	53.10 ± 0.07	30.41 ± 0.10	1.00
		0.40 ± 0.00	0.16 ± 0.00	49.09 ± 0.07	30.58 ± 0.10	1.00
		0.41 ± 0.00	0.18 ± 0.00	48.15 ± 0.06	30.82 ± 0.10	1.00
		0.41 ± 0.00	0.17 ± 0.00	50.42 ± 0.08	30.80 ± 0.10	1.00
		0.38 ± 0.00	0.16 ± 0.00	48.38 ± 0.11	40.30 ± 0.17	1.00

Table 2. Correlation analysis of the creep strain increment characteristic parameters.

Experimental Factor	Instantaneous Elasticity Modulus E_0/MPa	Hysteretic Elasticity Modulus E_r/MPa	Coefficient of Viscosity η/(MPa·s)	Relaxation Time τ_r/s
Cyclic loading times/times	0.648 **	0.890 **	0.339	0.408 *
Cyclic stress peak σ/MPa	0.893 **	0.952 **	0.241	0.841 **
Cyclic loading frequency f/Hz	−0.928 **	−0.924 **	−0.951 **	−0.771 **

Note: ** indicates that the difference is extremely significant ($p < 0.01$); * indicates that the difference is significant ($p < 0.05$).

3.2.1. Effect of Cyclic Loading Times on the Creep Performance of Machine-Harvested Seed Cotton

When the loading frequency was f = 6 Hz, the cyclic stress peak was σ = 0.113 MPa. The full creep strain curves of the machine-harvested seed cotton are shown in Figure 8a after cyclic loading. The full creep strain mechanism of the machine-harvested seed cotton is consistent with the increase in creep time, and they all show rapid growth first and then stability.

The initial creep strains of the machine-harvested seed cotton after different cyclic loading times are shown in Figure 8b. The aforementioned figure reveals that the initial creep strain of the machine-harvested seed cotton shows an overall increasing trend with increasing cyclic loading times under the same cyclic loading frequency and cyclic stress peak conditions, but some data fluctuate. In the cyclic loading process, the hysteresis curve deviated (Figure 4). The deviation increases with the cyclic loading times. Consequently, the initial creep strain shows an increasing trend. The data fluctuate because the machine-harvested seed cotton itself is a mixture containing cotton fiber, cotton seeds, impurities of the seed cotton itself (cotton stalk, cotton leaves, and boll shells), and other impurities (residual film, hair, etc.). In the compression process of the machine-harvested seed cotton, the internal arrangement of the cotton seeds and the type and amount of cotton impurities affect its stress and strain curve, showing the fluctuation of the initial creep strain.

The creep strain increment trend of the machine-harvested seed cotton in Figure 8c shows that the creep strain increment decreases with increasing cyclic loading times. This relationship occurs because more plastic deformation is generated, and plastic accumulates between seed cotton fibers with the increase in the cyclic loading times, resulting in a tighter fiber bond formed inside the machine-harvested seed cotton. Moreover, the internal clearance decreases, the friction inside the seed cotton and between the seed cotton and the chamber increases, and the degree of mutual slippage between the seed cotton fibers decreases, resulting in a reduction in the creep strain increment. Table 3 shows that the cyclic loading time has a considerable effect on the instantaneous elasticity modulus E_0 and hysteresis modulus E_r ($p < 0.5$), and the instantaneous elasticity modulus E_0 and hysteresis modulus E_r increase with increasing cyclic loading. The overall positive correlation is

shown, and the corresponding correlation coefficients are r = 0.924 and 0.942. The higher the modulus of elasticity E_0, the lower the elastic deformability. The higher the value of the viscosity coefficient η is, the higher the deformability resistance and the poorer the mobility of the internal structure of the machine-harvested seed cotton will be. Consequently, the instantaneous elastic modulus E_0 and hysteresis elastic modulus E_r increase, indicating that the more cyclic loading times, the smaller the instantaneous elastic deformability. Although the cyclic loading times in Table 2 are not significantly correlated with the viscosity coefficient η, Table 3 shows an overall upward trend for the viscosity coefficient η, indicating that the internal fluidity of the machine-harvested seed cotton is worse with the increase in the cyclic loading times. Thus, smaller creep strain increments are produced, generating better shape stability of the machine-harvested seed cotton after compression.

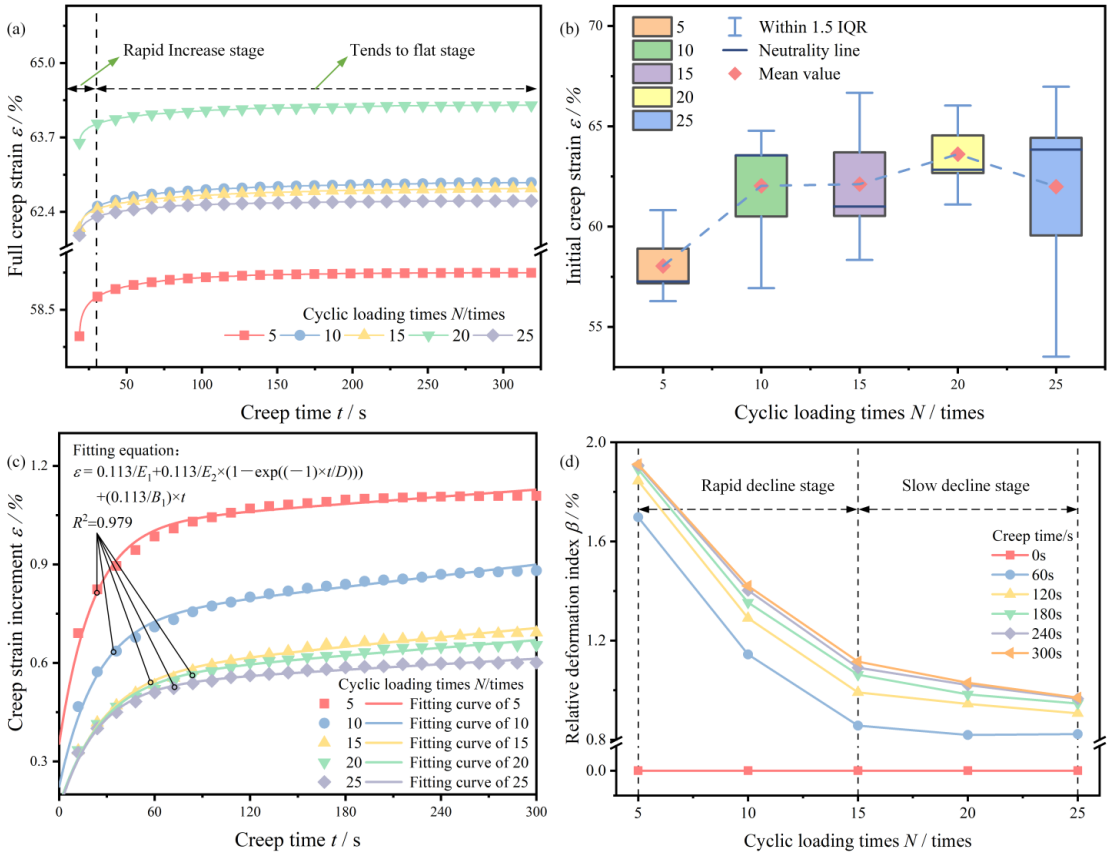

Figure 8. Full creep strain curve (**a**), initial creep strain (**b**), creep strain increment (**c**), and relative deformation index (**d**) of the machine-harvested seed cotton corresponding to the different cyclic loading times.

Table 3. ANOVA of creep parameters at different levels of cyclic loading times.

Cyclic Loading Times /times	Instantaneous Elasticity Modulus E_0/MPa	Hysteretic Elasticity Modulus E_r/MPa	Coefficient of Viscosity η/(MPa·s)	Relaxation Time τ_r/s
5	0.32 a	0.17 a	343.94 a	20.98 a
10	0.55 b	0.22 b	223.65 a	23.35 ab
15	0.74 b	0.28 c	277.56 a	28.09 ab
20	0.69 b	0.29 c	304.60 a	27.04 bc
25	0.76 b	0.30 c	493.67 a	23.98 c

Note: Different values after the same column of data indicate significant differences between data ($p < 0.05$). The same principle applies below.

The isochronous curves of the relative deformation index of the machine-harvested seed cotton with the cyclic loading times are shown in Figure 8d. The relative deformation index can be divided into two stages with increasing cyclic loading times when the creep times are the same. Furthermore, the relative deformation index of the machine-harvested seed cotton rapidly decreases with the increase in cyclic loading times in the fast-declining stage and the relative deformation index in the slow-declining stage. Although this stage achieves a smaller value, the overall trend is flatter than the previous stage mainly because the initial creep strain increases with the increase in the cyclic loading time, and the creep strain increment decreases. This result shows that the relative deformation index decreases, and the ability of the machine-harvested seed cotton to maintain the initial deformation increases. Moreover, increasing the cyclic loading times can improve the ability of the machine-harvested seed cotton to retain the initial deformation during creep. However, excessively increasing the cyclic loading times is insignificant for improving the ability of the machine-harvested seed cotton to maintain the initial deformation.

3.2.2. Effect of Cyclic Stress Peak on the Creep Properties of Machine-Harvested Seed Cotton

The curves of the full creep strain, initial creep strain, and creep strain increment with time for the different cyclic stress peaks are shown in Figures 9a, 9b, and 9c, respectively. Meanwhile, the isochronous curves of the relative deformation index of the cyclic stress peaks of the machine-harvested seed cotton are shown in Figure 9d.

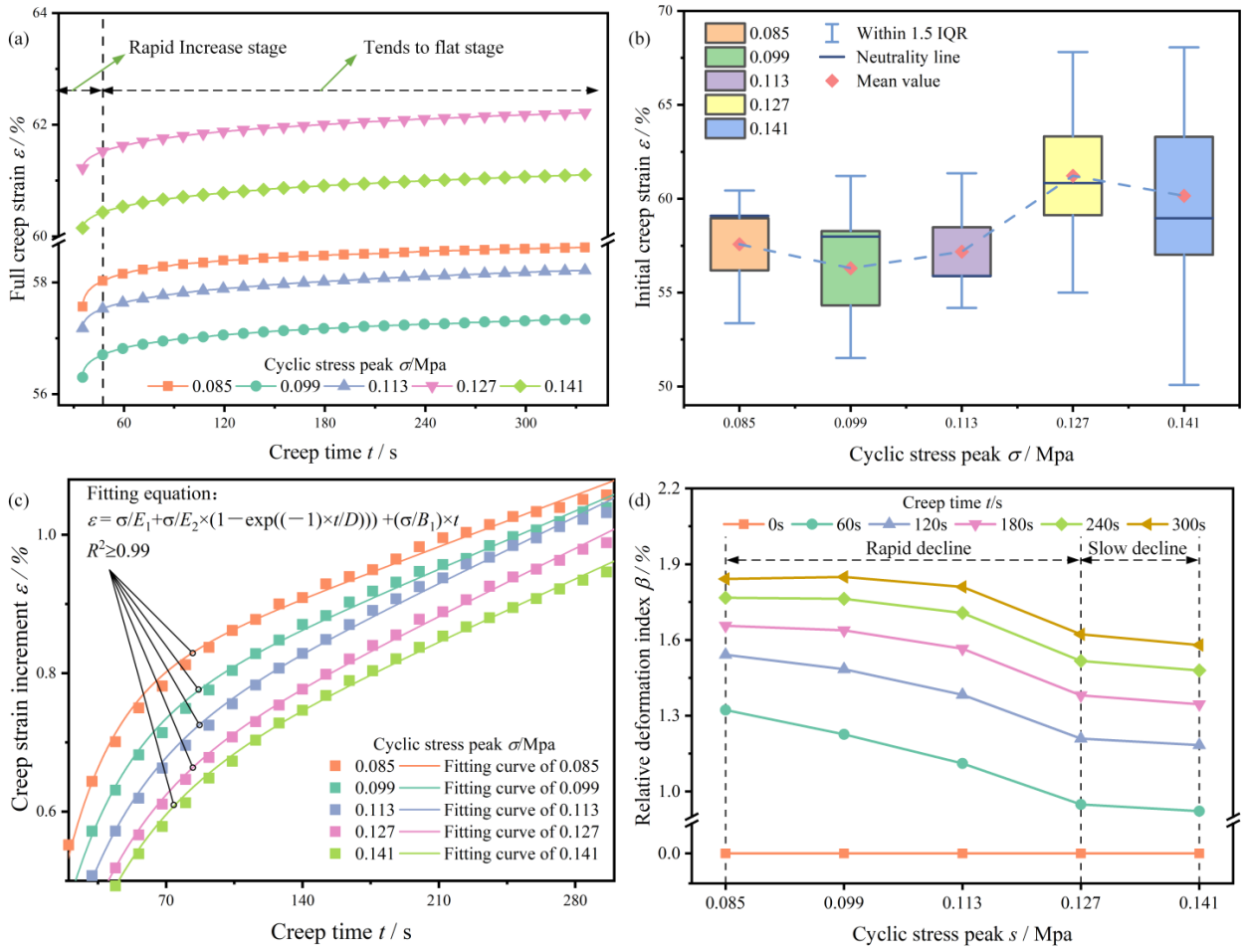

Figure 9. Full creep strain curve (**a**), initial creep strain (**b**), creep strain increment (**c**), and relative deformation index (**d**) of the machine-harvested seed cotton corresponding to the different cyclic stress peaks.

The trend of the machine-harvested seed cotton's full creep strain curve under different cyclic stress peak conditions is the same, showing a rapid increase before leveling off (Figure 9a). The initial creep strain of the machine-harvested seed cotton shows an overall increasing trend with the rise in cyclic stress peak, but some of the data have fluctuations (Figure 9b). This phenomenon arises because the higher cyclic stress peak produces a more significant displacement during cyclic loading. Thus, the initial creep strain increases. The reason for the fluctuation in the data is the same as above.

Figure 9c shows that the creep strain increment of the machine-harvested seed cotton shows an overall trend of gradually decreasing with the increase in the cyclic stress peak. This trend occurs because under the same cyclic loading frequency and cyclic loading times, the higher the stress peak produced, the closer the fiber bonding inside the machine-harvested seed cotton, and the greater the plastic deformation produced. However, the creep strain increment of the machine-harvested seed cotton is the smallest when the cyclic stress peak is σ = 0.085 MPa. The curve trend is also relatively flat compared with other curves, which is probably due to the arrangement of the internal cotton seeds and the uniform distribution of impurity species. Consequently, the machine-harvested seed cotton easily compresses and produces more plastic deformation; thus, a higher initial creep strain creates lower cyclic stress peaks. By contrast, the plastic deformation produced by low stress is limited, resulting in a relatively flat creep curve during pressure retention compared with other curves. The creep increment is relatively small.

The ANOVA results in Table 4 show that the effect of the cyclic stress peak on the instantaneous elasticity modulus E_0, hysteresis modulus E_r, and delay time τ_r of the machine-harvested seed cotton is significantly below the significance level of 0.05. Furthermore, the instantaneous elasticity modulus E_0, hysteresis modulus E_r, and delay time τ_r of the machine-harvested seed cotton increase with the increase in the cyclic stress peak, and the corresponding correlation coefficients are r = 0.893, 0.952, and 0.841, respectively. The instantaneous elasticity modulus E_0, hysteresis modulus E_r, and delay time τ_r increase, indicating that the higher the cyclic stress peak of the machine-harvested seed cotton generates, the smaller the transient elastic deformation in the creep phase, the poorer the internal mobility of the machine-harvested seed cotton, and the smaller the permanent deformation. Accordingly, a smaller creep strain increment is produced, which is more conducive to maintaining the shape stability of the machine-harvested seed cotton after compression. Similar results have been obtained in the relaxation process of the knitted cotton fabrics [29].

Table 4. ANOVA of the creep parameters at different levels of cyclic stress peak.

Cyclic Stress Peak σ/MPa	Instantaneous Elasticity Modulus E_0/MPa	Hysteretic Elasticity Modulus E_r/MPa	Coefficient of Viscosity η/(MPa·s)	Relaxation Time τ_r/s
0.085	0.45 a	0.16 a	96.25 a	25.15 a
0.099	0.49 ab	0.20 b	83.82 a	30.45 b
0.113	0.66 b	0.24 c	84.06 a	34.41 bc
0.127	0.95 c	0.28 d	94.22 a	35.78 c
0.141	1.15 d	0.31 e	114.54 a	38.43 c

The relative deformation index displayed a trend of rapid decrease, followed by a slight decline with the increase in the cyclic stress peak for the same creep time (Figure 9d). This trend is mainly due to the increase in the cyclic stress peak inducing the growth of the initial creep strain and the decrease in the creep strain increment. This result shows that the relative deformation index decreases, and the ability of the machine-harvested seed cotton to maintain the initial deformation increases, indicating that a moderate increase in the cyclic stress peak can enhance the retention ability of the initial creep strain of the machine-harvested seed cotton during creep. Nevertheless, an excessive increase in the

cyclic stress peak can no longer improve the initial deformation retention ability of the machine-harvested seed cotton to a significant extent.

3.2.3. Effect of Cyclic Loading Frequency on the Creep Performance of Machine-Harvested Seed Cotton

The full creep strain, initial creep strain, creep strain increment, and relative deformation index curves of the machine-harvested seed cotton for the different cyclic loading frequencies are shown in Figure 10 (i.e., when the cyclic stress peak is σ = 0.113 MPa, and the cyclic loading times are 15 times).

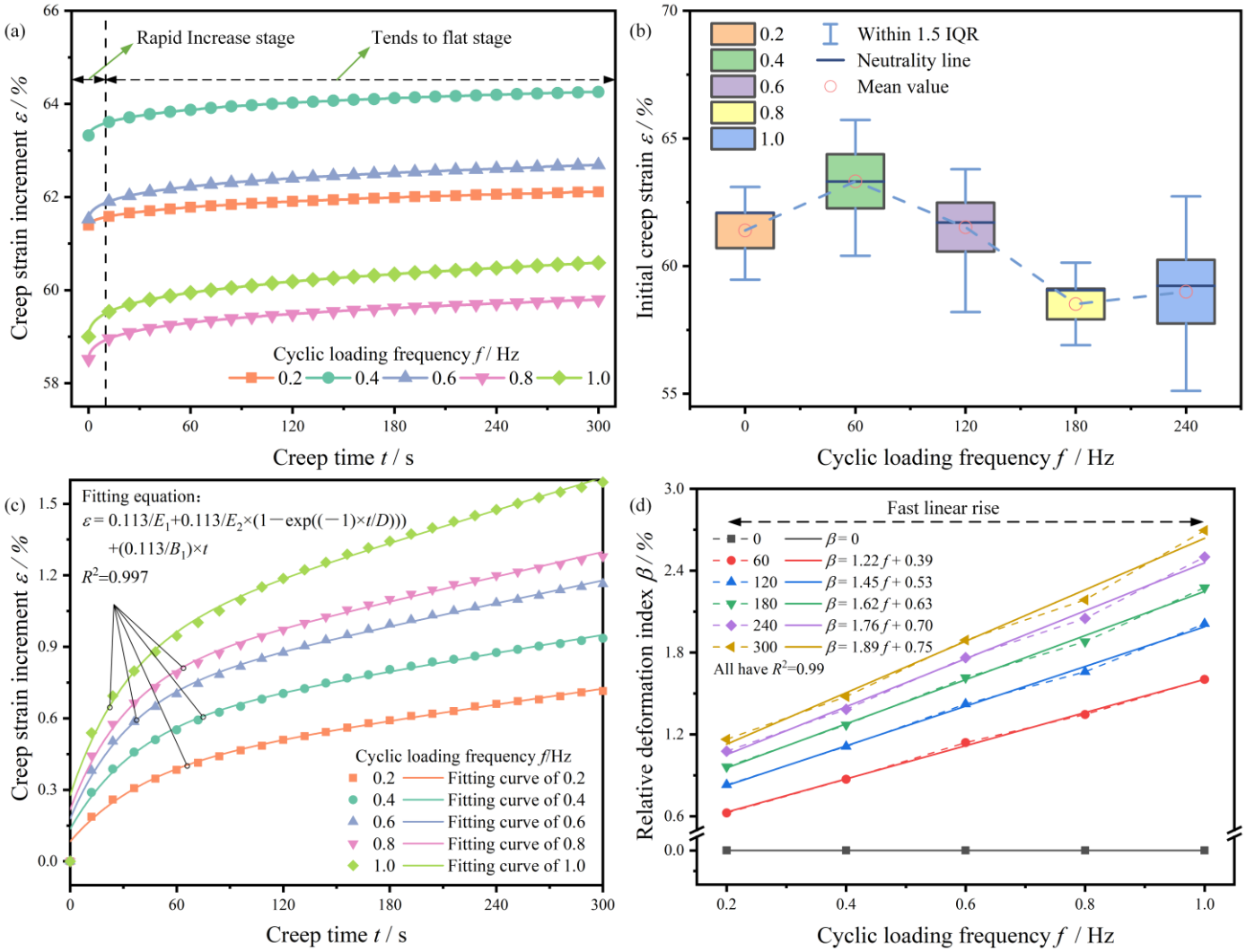

Figure 10. Full creep strain curve (**a**), initial creep strain (**b**), creep strain increment (**c**), and relative deformation index (**d**) of the machine-harvested seed cotton corresponding to the different cyclic loading frequencies.

Figure 10a shows that the full creep strain curves of the machine-harvested seed cotton under different cyclic loading frequencies are highly similar. These curves all show an overall trend of rapid increase and then leveling off. The initial creep strain of the machine-harvested seed cotton corresponds to the different cyclic loading frequencies (Figure 10b). This finding shows that the initial creep strain of the machine-harvested seed cotton exhibits a decreasing trend with the increase in the cyclic loading frequency. Nevertheless, some values fluctuate because a faster cyclic loading frequency results in a quicker corresponding loading speed and better air resistance, thus producing smaller

displacements and decreasing the initial creep strain. The reason for the fluctuation is the same as above.

Figure 10c shows that the creep strain increment of the machine-harvested seed cotton increases with increased cyclic loading frequency because increasing the loading frequency in the cyclic loading stage decreases the time of structural adjustment between the seed cotton fiber molecules. The degree of sufficient slip between fibers decreases. By contrast, the time of seed cotton springback is reduced during the unloading phase, and more structural adjustment is required. Therefore, the creep strain increment increases with increasing cyclic loading frequency.The ANOVA results in Table 5 show that the effect of the cyclic loading frequency on the instantaneous elasticity modulus E_0, hysteresis modulus E_r, coefficient of viscosity η, and delay time τ_r of the machine-harvested seed cotton is significantly below the significance level of 0.05. As shown in Table 2, the corresponding correlation coefficients are $r = -0.928$, -0.924, -0.951, and -0.771. The instantaneous elasticity modulus E_0, hysteresis modulus E_r, viscosity coefficient η, and delay time τ_r of the machine-harvested seed cotton decreased, indicating that the higher the cyclic loading frequency generates greater instantaneous elastic deformation in the creep phase, the better the internal mobility of seed cotton. The greater the mutual slip and adjustment of fibers produced, the greater the permanent deformation. Moreover, a more significant creep strain increment occurs, which is not conducive to maintaining the shape stability of the machine-harvested seed cotton after compression.

Table 5. ANOVA of the creep parameters at different levels of cyclic loading frequency.

Cyclic Loading Frequency f/Hz	Instantaneous Elasticity Modulus E_0/MPa	Hysteretic Elasticity Modulus E_r/MPa	Coefficient of Viscosity η/(MPa·s)	Relaxation Time τ_r/s
0.2	1.36 a	0.36 a	102.43 a	41.04 a
0.4	0.83 b	0.26 b	90.57 b	36.90 a
0.6	0.63 c	0.22 b	71.48 b	32.85 a
0.8	0.52 d	0.20 c	65.45 c	31.49 b
1.0	0.41 e	0.17 d	49.83 d	32.58 c

The isochronous curves of the relative deformation index of the machine-harvested seed cotton correspond to the cyclic loading frequency at different moments in Figure 10d. The relative deformation index of the machine-harvested seed cotton linearly increases with the cyclic loading frequency ($R^2 \geq 0.9898$) in the level range selected for this test. The increase in cyclic loading frequency is not conducive to improving the initial deformation retention ability of the machine-harvested seed cotton in the creep process. Although a low cyclic loading frequency can improve the deformation retention ability of the machine-harvested seed cotton in the creep process, it increases the time-consuming workload of the cyclic loading process before creep. Increasing the loading frequency can effectively reduce the time-consuming loading stage of the machine-harvested seed cotton. However, given the inertia of the instrument fixture, a transient overload phenomenon easily occurs in the cyclic loading process [22], thus affecting the test results. In addition, accurately controlling the initial creep stress of the machine-harvested seed cotton is not conducive.

4. Conclusions

In this experiment, machine-harvested seed cotton was regarded as the research object. The test factors used were the cyclic loading time, cyclic stress peak, and cyclic loading frequency. The energy change during the cyclic loading process of the machine-harvested seed cotton, the creep characteristics during the creep process, and the ability to maintain the initial creep strain were analyzed and characterized by a single factor. The energy consumption curve of the machine-harvested seed cotton during cyclic loading was obtained to analyze its energy change law. The full creep strain was divided into two

parts: initial creep strain and creep strain increment, and the relative deformation index was introduced to characterize its deformation retention capacity. The main conclusions are as follows:

1. Machine-harvested seed cotton shows hysteresis characteristics in the cyclic loading-and-unloading process. The loading and unloading curves of the machine-harvested seed cotton in the cyclic loading process are similar in shape and consistent in law. The compression energy could be expressed as an exponential function ($R^2 \geq 0.91$) with increased cyclic loading times. The compression energy in the loading stage of the machine-harvested seed cotton rapidly decreases and then stabilizes with the increase in the cyclic loading times. The compression energy in the compression process of the machine-harvested seed cotton increases with the rise in the cyclic stress peak cyclic loading frequency.

2. After cyclic loading under different conditions, the creep strain curves of machine-harvested seed cotton are similar in shape, and the creep mechanisms are consistent, showing a general trend of rapidly increasing and then leveling off. The initial creep strain of machine-harvested seed cotton shows an overall increasing trend with the increase in cyclic loading times and cyclic stress peak. By contrast, the initial creep strain shows a general decreasing trend with the increase in cyclic loading frequency.

3. Cyclic loading time, cyclic stress peak, and cyclic loading frequency have different effects on the instantaneous elasticity modulus E_0, hysteresis modulus E_r, viscosity coefficient η, and delay time τ_r of machine-harvested seed cotton. The creep strain increment decreases with increasing cyclic loading times. Moreover, the instantaneous elastic modulus E_0 and the hysteresis elastic modulus E_r increase, and the relative deformation index decreases. The creep strain increment shows a decreasing trend with the increase in the cyclic stress peak. The instantaneous elastic modulus E_0, hysteresis elastic modulus E_r, and delay time τ_r increase, but the relative deformation index decreases. The creep strain increment increases with the increase in cyclic loading frequency. The instantaneous elastic modulus E_0, hysteresis elastic modulus E_r, viscosity coefficient η, and delay time τ_r decrease, and the relative deformation index linearly increases.

4. Without considering the power consumption and interaction, appropriately increasing the cyclic loading times and the peak cyclic loading stress and minimizing the cyclic loading frequency can reduce the relative deformation index of the creep phase of machine-harvested seed cotton. Accordingly, the deformation retention ability of machine-harvested seed cotton in the creep process decreases, but the compression energy increases.

Author Contributions: Conceptualization, X.W. and H.Z.; methodology, X.W. and M.W.; software, X.W.; validation, L.W., X.D. and L.C.; formal analysis, M.W.; investigation, S.Z.; resources, H.Z.; data curation, X.W. and M.W.; writing—original draft preparation, X.M; writing—review and editing, M.W.; visualization, X.D.; supervision, L.C.; project administration, H.Z., L.W. and M.W.; funding acquisition, H.Z., L.W. and M.W. All authors have read and agreed to the published version of the manuscript.

Funding: This study was funded by three projects, including the National Natural Science Foundation (Project No. 32260435), the Corps Key Field Innovative Team Building Project (Project No. 2019CB006), and the Shihezi University Youth Innovation Cultivation Talent Project (Project No. CXPY202120).

Institutional Review Board Statement: Not applicable.

Informed Consent Statement: Not applicable.

Data Availability Statement: All relevant data presented in the article are stored according to institutional requirements and, as such, are not available online. However, all data used in this manuscript can be made available upon request to the authors.

Conflicts of Interest: The authors declare no conflicts of interest.

References

1. Yuan, Y.; Bai, S.; Niu, K.; Zhou, L.; Zhao, B.; Wei, L.; Liu, L. Research progress in the key technologies and equipment for cotton planting mechanization. *Trans. Chin. Soc. Agric. Eng.* **2023**, *39*, 1–11. [CrossRef]
2. China. Xinjiang Cotton Production Accounted for 90.2% of the National Record High. 2022. Available online: http://www.gov.cn/xinwen/2022-12/27/content_5733816.htm (accessed on 20 December 2023).
3. Chen, X.; Wen, H.; Zhang, W.; Pan, F.; Zhao, Y. Advances and progress of agricultural machinery and sensing technology fusion. *Smart Agric.* **2020**, *2*, 1. [CrossRef]
4. Bidour, A.; Fatma, G.; Marianna, H. A new method in fabric drape measurement and analysis of the drape formation process. *Text. Res. J.* **2011**, *82*, 502–512. [CrossRef]
5. Zou, Z. A Brief Discussion on the Development of Machine Picking Cotton in Xinjiang Corps. *China Fiber Insp.* **2020**, *1*, 33. [CrossRef]
6. Kong, F.; Wu, T.; Chen, C.; Sun, Y.; Xie, Q.; Shi, L. Mechanical properties and construction of constitutive model for compression and stress relaxation of seed cotton. *Trans. Chin. Soc. Agric. Eng.* **2021**, *37*, 53–60. [CrossRef]
7. Wang, J.; Zhang, H.; Wang, L.; Wei, X.; Wang, M.; Gu, Y.; Cai, Y. Experimental Study and Simulation of the Stress Relaxation Characteristics of Machine-Harvested Seed Cotton. *Appl. Sci.* **2021**, *11*, 9959. [CrossRef]
8. Hardin, R.G., IV; Searcy, S.W. Modeling of seed cotton viscoelastic properties. *Trans. ASABE* **2009**, *52*, 707–714. [CrossRef]
9. John Deere. Available online: https://www.deere.com/en/harvesting/cotton/ (accessed on 20 January 2024).
10. Tang, Z.; Liang, Y.; Zhang, B.; Wang, M.; Hao, Z.; Li, Y. Effects of multi-sequence combination forces on creep characteristics of bales during wheat harvesting. *Int. J. Agric. Biol. Eng.* **2021**, *14*, 88–99. [CrossRef]
11. Peng, H.; Salmén, L.; Jiang, J.; Lu, J. Creep properties of compression wood fibers. *Wood Sci. Technol.* **2020**, *54*, 1497–1510. [CrossRef]
12. Chen, J.; Zhao, N.; Fu, N.; Li, D.; Wang, L.; Chen, X. Mechanical properties of hulless barley stem with different moisture contents. *Int. J. Food Eng.* **2019**, *15*, 1–10. [CrossRef]
13. Xiao, J.; Ma, R.; Chen, Y. Effects of test levels on creep and relaxation characteristic parameters of stem for rice seedlings grown in plastic cell tray. *Int. J. Agric. Biol. Eng.* **2020**, *13*, 19–28. [CrossRef]
14. Graham, V.; Bilanski, W. Non-linear viscoelastic behavior during forage wafering. *Trans. ASAE* **1984**, *27*, 1661–1665. [CrossRef]
15. Nielsen, S.; Rezaei, H.; Mandø, M.; Shahab, S. Constitutive modelling of compression and stress relaxation in pine pellets. *Biomass Bioenergy* **2019**, *130*, 105370. [CrossRef]
16. Du, X.; Guo, W.; Wang, C.; Wang, H.; Jin, M.; Liu, X.; Li, J. Stress relaxation characteristics and parameters optimization of feed sweet sorghum. *J. China Agric. Univ.* **2019**, *24*, 123–131. [CrossRef]
17. Ma, Y. Analysis of Rheological Properties and Microstructure of Biomass Compact Molding Under Vibration Force Field. Doctor degree, Inner Mongolia Agricultural University, Hohhot, China, 2015.
18. Li, Y.; Li, Y.; Chen, Y.; Su, X.; Liu, W. Change Laws of Energy Consumption of Cotton in the Successive Loading Mode. *Anhui Agric. Sci.* **2020**, *48*, 182–185. [CrossRef]
19. Wang, R.; Wei, K.; Liu, Y.; Chen, Z.; Ma, F.; Liu, D. Optimization of process parameters for multi-frequency rapid compression molding of corn stalk silk used for forage. *Trans. Chin. Soc. Agric. Eng.* **2016**, *32*, 277–281. [CrossRef]
20. Zhao, G.; Wang, C.; Han, X.; Fan, L. Study on creep properties of alfalfa. *Agric. Mech. Res.* **2009**, *31*, 121–124.
21. Li, X.; Xiong, S.; Geng, L.; Ji, J. Influence of water content on anti-pressing properties of corn ear. *Trans. Chin. Soc. Agric. Eng.* **2018**, *34*, 25–31. [CrossRef]
22. Wang, Z.; Li, S.; Tan, D.; Meng, S.; He, B. Effect of cyclic loading treatment on creep behavior of polyvinyl chloride coated membrane. *J. Text. Res.* **2021**, *42*, 101–107. [CrossRef]
23. Wang, J.; Zhang, H.; Wang, L.; Wei, X.; Gu, Y.; Zhang, L.; Cai, Y. Study on Compression Characteristics and Compressibility of Machine-harvested Seed Cotton. *Acta Agric. Univ. Jiangxiensis (Nat. Sci. Ed.)* **2022**, *44*, 212–221. [CrossRef]
24. Nakajima, C.; Yoneda, M. Compressive Stress Relaxation and Creep Properties of Synthetic Fiber and Regenerated Fiber Assemblies. *J. Text. Eng.* **2012**, *56*, 139–146. [CrossRef]
25. Li, Y.; Wang, X.; Xu, L. Effect of loading/unloading times on mechanical damage of rice grains. *Trans. Chin. Soc. Agric. Mach.* **2007**, *10*, 61–63+76.
26. Du, X.; Mao, H.; Wang, C. Compression characteristics and the influencing factors of sweet sorghum straw: Experimental study. *BioRes* **2020**, *15*, 9429–9443. [CrossRef]
27. Yang, M. *Rheology of Agricultural Materials*; China Agriculture Press: Beijing, China, 2010.
28. Qiu, S.; Yuan, X.; Guo, Y.; Cui, Q.; Wu, X.; Zhang, Z. Effects of variety and moisture content on mechanical properties of millet. *Trans. Chin. Soc. Agric. Eng.* **2019**, *35*, 322–326. [CrossRef]
29. Marzougui, S.; Zaouali, R.; Shafee, W. Energy Model for Describing the Viscoelastic Behavior of Knitted Cotton Fabric During Relaxation. *Fibers Polym.* **2023**, *24*, 1149–1156. [CrossRef]